Electronic excitation of H_2 in slow collisions with molecular ions

M. Krishnamurthy, Peter Gross, and D. Mathur
Tata Institute of Fundamental Research, Homi Bhabha Road, Bombay 400 005, India
(Received 8 April 1994)

Excitation of molecular hydrogen has been studied in 1.8-keV collisions with molecular projectile ions H_2^+, N_2^+, CO^+, O_2^+, and CO_2^+ by means of energy-loss spectrometry using a high-resolution ion translational energy spectrometer. Excitation of the target H_2 is observed only in the case of collisions with H_2^+. Oscillator strengths for electronic transitions to various electronic states are determined by simulating the measured energy-loss spectra with calculations using calculated Franck-Condon overlap integrals. Excitation of the projectile ions is observed in the case of collisions with N_2^+ and CO^+ projectiles. Neither projectile excitation nor target excitation is observed when experiments are carried out with O_2^+ and CO_2^+ projectiles. The results obtained in the present study are interpreted as a manifestation of wave-function-overlap effects involving the highest occupied molecular orbitals of the target and projectile ions.

PACS number(s): 33.90.+h, 34.90.+q, 35.20.Wg

I. INTRODUCTION

Molecular hydrogen has been of importance in the study of many quantum mechanical phenomena. Although it is the simplest two-centered system with two electrons, quantitative insights into the physics of collisional interactions of H_2 with heavy particles have been inhibited by a relative paucity of experimental information. Some attention has been focused on H_2 as a model system for the study of dissociative ionization induced by heavy particle impact [1] and electronic excitation [2,3]. In the case of H_2, both these processes assume particular importance from the viewpoint of important applications in astrophysics. For low-energy ion-molecule collisions, cross sections for electron capture from H_2 are two orders of magnitude lower than for other diatomic molecules such as N_2, CO, and O_2, and it is electronic excitation (collisional as well as radiative) that is an important process which governs the abundance of H_2 in interstellar gas clouds [4] and which contributes to the opacity in stellar atmospheres [5]. Excitation from the $X\,^1\Sigma_g^+$ ground state of H_2 into vibrational levels of the $B\,^1\Sigma_u^+$ and $C\,^1\Pi_u$ states, corresponding to the Lyman and Werner systems, respectively, and the subsequent downward transitions to the vibrational continuum of the ground state constitute the primary destruction mechanism for H_2 in the interstellar medium [6], leading to heat generation via production of energetic H atoms.

It is clear that experimental studies of collisional excitation of H_2, including determinations of oscillator strengths, are of considerable contemporary interest, particularly insofar as development of new models of the time-dependent evolution of interstellar clouds and their energy budget are concerned. However, such studies have been limited in the extreme [7]. In the present work, we report results of high-resolution translational energy spectrometry experiments on the excitation of the H_2 molecule in 1.8-keV collisions with the molecular projectile ions H_2^+, N_2^+, CO^+, O_2^+, and CO_2^+ ions. Excitation of molecular hydrogen from the ground state $X\,^1\Sigma_g^+$ to $b\,^3\Sigma_u^+$ $B\,^1\Sigma_u^+$, $C\,^1\Pi_u$, $e\,^3\Sigma_u^+$, $D\,^1\Pi_u$, and $D'\,^1\Pi_u$ states and the ionic state $X\,^2\Sigma_g^+$ of H_2^+ are observed only in the case of collisions between H_2 and H_2^+ ions. Excitation of the projectile ions is observed in collisions of H_2 with the N_2^+ and CO^+ ions. Neither projectile excitation nor target excitation is observed in the case of collisions with O_2^+ and CO_2^+ projectile ions. These results are explained in terms of simple molecular orbital arguments and energy considerations.

In very recent studies that we have conducted on the collisional excitation of other neutral diatomic molecules (such as CO, N_2, and NH_3) by molecular ion projectiles [8–10], it has been found that the cross section for collisional excitation of target molecules was sensitively dependent on the quantal description of the projectile ions used. The excitation cross sections were found to directly depend on the overlap integrals of the highest occupied molecular orbitals (HOMO's) of the two colliding systems. For target molecules such as N_2 and CO, which possess $^1\Sigma$ symmetry in their ground electronic state, the excitation cross sections were substantially larger in the case of collisions with projectile ions having $^2\Sigma$ symmetry; in such instances, the overlaps between the HOMO's of the projectile and target are large. However, in collisions with projectile ions possessing $^2\Pi$ symmetry, such as CO_2^+ and CS_2^+, the excitation cross sections were shown to be at least an order of magnitude lower as the corresponding overlaps of the HOMO's are considerably smaller in such cases.

In any collisional interaction between ions and neutral molecules, the perturbation of the neutral target molecule with the projectile ion leads to the collisional excitation of the former. However, in perturbing the target molecules, the projectile ion is also perturbed and could also undergo excitation to various electronic states. If the vertical excitation energy of the target molecule is much larger than the dissociation energy of the projectile ions, then collisions leading to excitation of the target

molecule and the projectile ion could result in dissociation of the projectile ion. Since the energy-loss spectra discussed here are obtained by monitoring the change in the kinetic energy of the projectile ions, such events resulting in the dissociation of the projectile ions are not recorded. Collision experiments with molecular hydrogen depict such a situation. The vertical excitation energy of even the lowest-lying excited electronic state $b\,^3\Sigma_u{}^+$ is about 10 eV, which is larger than the dissociation energy of most diatomic molecular ions. This consideration makes H_2 a particularly apt choice for a model system to probe wave-function overlap effects in collisional excitation by molecular projectile ions.

II. EXPERIMENTAL DETAILS

The experiments reported here were carried out on a high-resolution, multisector, ion translational energy spectrometer described in detail elsewhere [11]. Briefly, ions produced in a low-pressure electron impact ion source operated at a pressure of about 10^{-6} Torr are accelerated by an electrostatic potential of 1.8 kV and collimated into a thin pencil beam by a three-element einzel lens system. Mass selection of these ions is carried out by means of a crossed electric and magnetic field sector (Wien filter). The mass-selected ions are energy monochromatized using a large, cylindrical, 90° sector electrostatic analyzer of 55 cm mean radius. The energy-monochromatized ions are then made to collide, under single collision conditions, with the neutral target molecules in a collision cell maintained at a pressure of about 5×10^{-4} Torr. The forward-scattered ions are then energy analyzed with another identical 90°, cylindrical electrostatic sector analyzer. The energy-analyzed projectile ions are detected by a channel electron multiplier operating in the pulse counting mode.

The overall energy resolution that can be obtained depends on the widths of the entry and exit slits of the two energy analyzers. With the large radius of the sector analyzers used, our instrument is capable of energy resolving powers in excess of 2×10^4 in the laboratory frame. The entry and the exit slits are varied to get the optimum energy resolution and the intensity of the projectile ions participating in the inelastic collisional excitation process. The angular resolution in the present experiment is about 0.1°, so that the energy-loss spectra discussed in this paper yield information on differential excitation cross sections at a scattering angle of about 0.0±0.1°. The ions traverse a distance of about 3 m before they are detected by the channel electron multiplier.

Being a low-pressure ion source, ions are produced in the ground electronic state as well as in low-lying excited states which may have a lifetime long enough to ensure that the projectile beam incident on the target molecule contains an unknown mixture of ground and excited electronic states. However, by judicious choice of the gas pressure in the ion source and the electron energy, we can eliminate significant contamination of the projectile ion beam by excited state species: the presence of projectile ions in long-lived excited electronic manifests itself in our apparatus as additional peaks in our translational energy spectra which can be readily identified. Operating conditions were chosen such that such peaks were totally eliminated from measured spectra in the present study. Vibrationally excited states in the projectile ion beam have not been taken into account in the analysis of the structure observed in the energy loss spectra measured in the present experiments.

III. RESULTS AND DISCUSSION

Figure 1(a) depicts a typical energy-loss spectrum obtained in the 1.8-keV collisions of projectile $H_2{}^+$ ions with molecular hydrogen. The intensity of the scattered $H_2{}^+$ is plotted as a function of the energy lost from the elastically scattered projectile molecular ions at 0° scattering angle. The energy loss is due to the collisional excitation of the molecular hydrogen target from the ground electronic state $^1\Sigma_g{}^+$ to a whole range of excited electronic states up to the ionic state $^2\Sigma_g{}^+$. Figure 1(b) shows the different potential-energy functions of the electronic states accessed in the collisional excitation. The potential-energy functions are obtained from calculations using spectroscopic information by the Rydberg-Klein-Rees method [12]. The two vertical lines in Fig. 1(b) represent the Franck-Condon transition region from the zeroth vibrational level of the ground electronic state $^1\Sigma_g{}^+$. The energy-loss envelope obtained in the collision

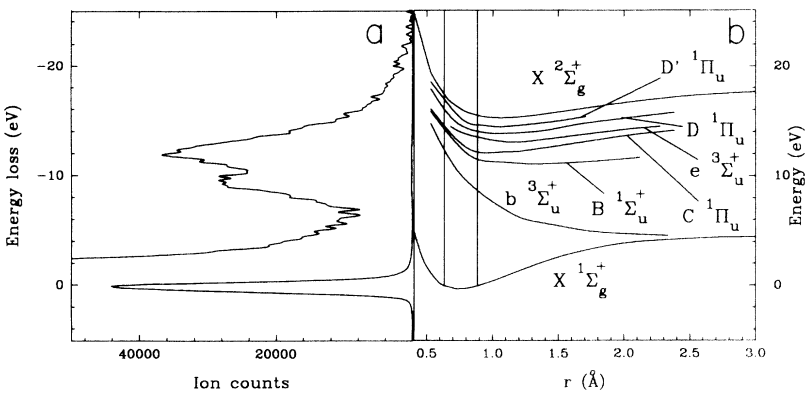

FIG. 1. Energy-loss spectrum of forward-scattered $H_2{}^+$ ions at 1.8-keV incident energy colliding with H_2 molecules (left panel) and the potential-energy functions of the different electronic states of H_2 and $H_2{}^+$ accessed during collisional excitation (right panel). The vertical lines in the right panel indicate the Franck-Condon region for transitions from the zeroth vibrational level of the ground electronic state $^1\Sigma_g{}^+$ of H_2.

of H_2^+ with H_2 is completely attributed to the excitation of the target H_2 molecule. This is because all the excited states of H_2^+ are purely repulsive and any excitation of the projectile ion would therefore lead to the dissociation of the projectile and subsequently such an event would not be recorded in our energy-loss spectrum.

The first excited state $b\,^3\Sigma_u^+$ of H_2 is purely repulsive. At somewhat higher excitation energies there lie a large number of bound excited states wherein an electron from the $1s\sigma$ orbital is excited to different orbitals in the third and fourth shells, etc., converging to the $^2\Sigma_g^+$ state of H_2^+. Doubly excited states of configuration H_2^{+**} $(2p\sigma^2)$ and $(2p\sigma 2p\pi)$ occur are expected to occur at higher values of energy loss (25–34 eV and 28–38 eV, respectively) lie outside the range covered in present experiments. Due to the large number of closely lying excited states it is not possible to directly resolve the energy-loss envelope obtained in the spectrum shown in Fig. 1(a). However, more information can be obtained by mathematically simulating [8] the measured energy-loss envelope in the manner described below.

Table I lists the different states to which electronic excitation from the ground state $^1\Sigma_g^+$ is considered, along with the range of energy-loss values for vertical excitation to the different vibrational states of the respective electronic states. Excitation to all the possible excited electronic states are considered in the simulation exercise we carried out. The collision times in our experiment are at least an order of magnitude smaller than the vibrational periods, so the transitions are considered to be purely Franck-Condon. The electronic transition energies and the Franck-Condon factors for excitation to the different vibrational states of the electronic states are obtained by using the semiclassical WKB approximation [13].

In the case of excitation to the $b\,^3\Sigma_u^+$ state, which is a purely repulsive state, the application of the WKB approximation to obtain the excitation function is not simple and straightforward. Excitation to this repulsive state is therefore dealt with by us using two different methods. The first method utilizes the so-called reflection principle, in which the continuum state wave function is considered to be a delta function at the classical turning point (r_e) [14,1,15]:

$$\psi_k \propto \delta(r - r_e), \tag{1}$$

where r is the internuclear distance. The excitation function is thus obtained by reflecting the zeroth vibrational state wave function of the ground electronic state $^1\Sigma_g^+$ on to the repulsive potential function of the $b\,^3\Sigma_u^+$ state.

In the second method the excitation function is obtained by using time-dependent wave-packet dynamics [16]. This method has been successfully applied by Henriksen *et al.* [17] to explain the photoabsorption spectra of H_2O. The excitation function $I(\omega)$ in this method is given by the Fourier transform of the autocorrelation function

$$I(\omega) \propto \int_{-\infty}^{\infty} \langle\psi(t)|\psi(0)\rangle e^{-i\omega t} dt, \tag{2}$$

where ω is the frequency and $\psi(0)$ is the initial wave packet at time $t = 0$, which is taken to be the zeroth vibrational wave function of the ground electronic state $^1\Sigma_g^+$ of H_2. $\psi(t)$ is the evolving wave packet at time t on the excited state potential function. $\psi(t)$ is computed by numerically propagating the Schrödinger equation in a series of discretized time steps Δt

$$\psi(t + \Delta t) = e^{-i\hat{H}\Delta t/\hbar}\psi(t), \tag{3}$$

where

$$\hat{H} = -\frac{\hbar^2}{2\mu}\frac{\delta^2}{\delta r^2} + V(r) \tag{4}$$

and r is the internuclear distance. We employ the split-operator method to evaluate (3) and perform the exponentiation of the kinetic-energy operator via the fast Fourier transform method as described in detail elsewhere [18]. The total propagation time is chosen to be long enough such that most of the initial wave packet $\psi(0)$ has propagated down into the asymptotic region of the repulsive potential function. We have added an optical (imaginary absorbing) potential to the Hamiltonian, which absorbs the wave packet once it has gone into the asymptotic region in order to avoid large coordinate sizes in our propagation method [19].

The total absorption spectrum obtained by this method has been shown to be totally equivalent to the golden rule expression for the total absorption spectrum [17]

$$I(\omega) \propto \sum_n |\langle E, n|\psi(0)\rangle|^2, \tag{5}$$

where n denotes all the quantum numbers needed to fully specify the state at energy E.

TABLE I. Energy-loss values for the excitation of H_2 in the process $H_2^+ + H_2 \rightarrow H_2^+ +$ product. ΔE denotes the range of energy-loss values expected from vertical excitation to the different vibrational levels of the excited states.

Product	ΔE (eV)
$B\,^1\Sigma_u^+$	11.18–13.95
$c\,^3\Pi_u$	11.77–13.01
$a\,^3\Sigma_g^+$	11.78–14.03
$C\,^1\Pi_u$	12.28–13.94
$e\,^3\Sigma_u^+$	13.24–14.49
$E, F,^1\Sigma_g^+$	12.29–12.83
$B'\,^1\Sigma_u^+$	13.70–14.62
$B''\,^1\Sigma_u^+$	14.50–15.61
$d\,^3\Pi_u$	13.85–16.36
$i\,^3\Pi_g$	13.87–14.61
$h\,^3\Sigma_g^+$	13.85–14.92
$g\,^3\Sigma_g^+$	13.89–14.95
$V\,^1\Pi_u$	14.57–16.48
$j\,^3\Delta_g$	13.94–16.50
$m\,^3\Sigma_u^+$	14.32–16.07
$D\,^1\Pi_u$	13.99–15.41
$D'\,^1\Pi_u$	14.61–16.21
$H_2^+\ X^2\Sigma_g^+$	15.41–17.33

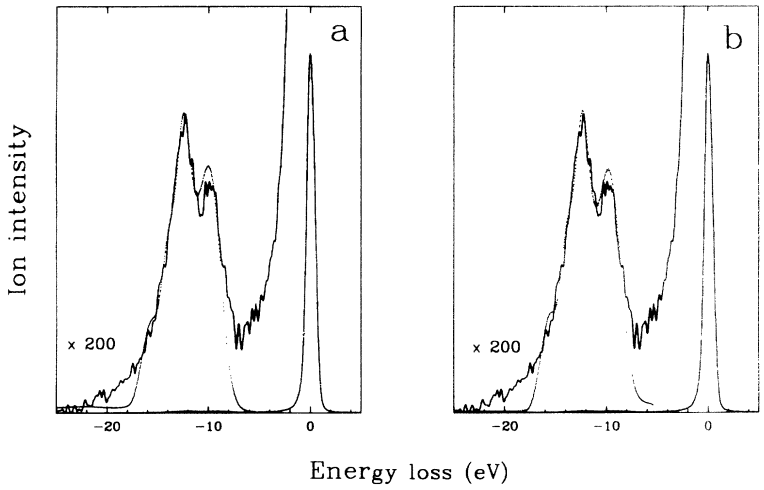

FIG. 2. (a) Energy-loss spectrum of H_2^+-H_2 collisions (solid curve) in comparison with the simulated curve (dotted line). The Franck-Condon integral for the excitation to the continuum state $^3\Sigma_u^+$ is calculated by the reflection approximation. (b) Energy-loss spectrum of H_2^+-H_2 collisions (solid curve) in comparison with the simulated curve (dotted line) when the Franck-Condon integral for the excitation to the continuum state $^3\Sigma_u^+$ is calculated by using the time-dependent wave-packet method.

To obtain the transition intensity, we then convolute the instrument function (which is essentially dominated by the transmission properties by the post-collision energy analyzer and is obtained experimentally by measuring the energy profile of the projectile ion beam with no collision gas) with an oscillator strength parameter and the Franck-Condon factors (for excitation to bound states) or the excitation function $I(\omega)$ in the case of the excited states that are repulsive. By varying the oscillator strength parameter, the energy-loss peak is simulated to fit the experimentally observed spectral peak shape. The fitting was found to improve when excitation to some of the triplet states and high-lying excited states (such as $V\,^1\Pi_u$ etc.) were not considered. This can be understood because the probability of excitation to these optically forbidden states is expected to be small.

Figure 2 shows the simulated spectra that best fit the experimentally observed energy-loss spectra. In Fig. 2(a), the simulated spectrum (shown as the dotted line) was obtained when the excitation function for the repulsive state $b\,^3\Sigma_u^+$ was calculated using the reflection approximation. The solid line shows the energy-loss envelope measured when 1.8-keV H_2^+ ions underwent single collisions with molecular hydrogen. Figure 2(b) shows the simulated spectrum obtained when the excitation function for the repulsive state was calculated by the time-dependent wave-packet dynamics method (dotted line), in comparison with the experimental energy-loss envelope (solid line). It is clear from a comparison of Figs. 2(a) and 2(b) that the excitation function obtained by the reflection approximation is very similar to the excitation function obtained using the more rigorous time-dependent calculations, although the fitting to the experimental spectrum is better with the latter technique. The time-dependent wave-packet approach is, however, more general and can be applied to cases where the excited state may be pre-dissociating rather than being purely repulsive, while the reflection approximation would be of little value in such a case. Furthermore, we note that, unlike the reflection approximation approach, the wave-packet approach is easily extended to multidimensional potential functions.

Table II displays the different electronic states which are required to obtain the best fit for the experimentally

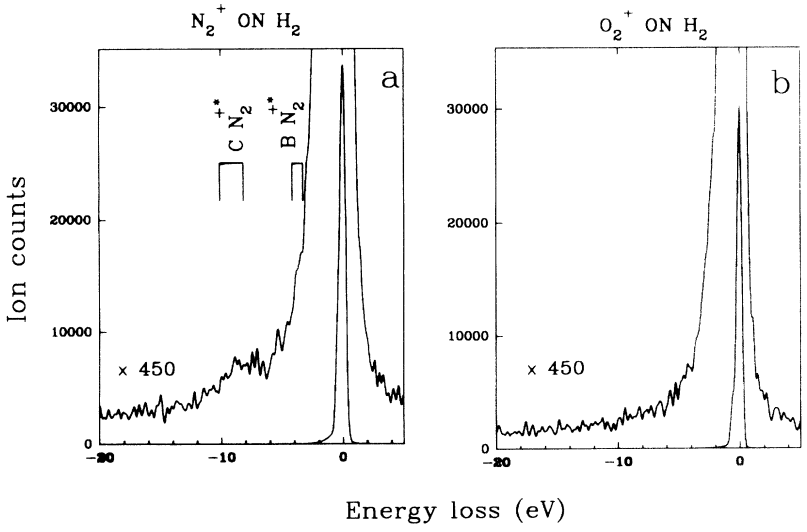

FIG. 3. (a) Energy-loss spectrum of N_2^+ ions colliding with H_2 molecules. The excitation energy for vertical excitations to the $B\,^2\Sigma_u^+$ and $C\,^2\Sigma_u^+$ states of N_2^+ are indicated in the top portion of the figure. (b) Energy-loss spectrum of O_2^+ colliding with H_2 molecules.

TABLE II. Relative oscillator strengths f_1^{nm} and f_2^{nm} for collisional excitation from the zeroth vibrational level of the $X\,^1\Sigma_g{}^+$ ground electronic state of H_2 to various electronic states of H_2 and $H_2{}^+$, when the excitation function for excitation to the repulsive state $^3\Sigma_u{}^+$ is calculated using the reflection approximation and time-dependent wave-packet dynamics formalism, respectively.

State	f_1^{nm}	f_2^{nm}
$b\,^3\Sigma_u{}^+$	0.47	0.41
$B\,^1\Sigma_u{}^+$	0.66	0.80
$C\,^1\Pi_u$	0.71	0.73
$e\,^3\Sigma_u{}^+$	0.38	0.50
$D\,^1\Pi_u$	0.46	0.46
$D'\,^1\Pi_u$	0.04	0.07
$H_2{}^+\ X\,^2\Sigma_g{}^+$	0.41	0.46

observed energy loss profile shown in Fig. 2, along with the relative oscillator strength parameters, which give the best fit. f_1^{nm} and f_2^{nm} represent the oscillator strengths for the excitation to the different electronic states, when the excitation function for the repulsive state $b\,^3\Sigma_u{}^+$ is calculated using the reflection approximation and time-dependent formalism, respectively. The differences in values of f_1^{nm} and f_2^{nm} reflect the different fits between measured and simulated spectra.

When collisional excitation studies similar to the $H_2{}^+$-H_2 collisions were carried out with $N_2{}^+$ projectile ions, the observations were quite different. Figure 3(a) shows the energy-loss spectra obtained in 1.8-keV collisions of $N_2{}^+$ with neutral H_2. The energy-loss profile expected to appear at about 10 eV (similar to the profile observed in Fig. 1) due to the electronic excitation of the target H_2 is totally absent. However, energy-loss due to the excitation of the projectile $N_2{}^+$ ions from the ground electronic state $^2\Sigma_g{}^+$ to the excited electronic states $B\,^2\Sigma_u{}^+$ and $C\,^2\Sigma_u{}^+$ are apparent in the spectrum. The energy-loss values expected [20] due to these transitions are marked in the top portion of Fig. 3(a). However, when experiments were carried out with $O_2{}^+$ and $CO_2{}^+$ projectile ions, energy-loss due to either excitation of the projectile ions or target excitation is absent. This is demonstrated in Fig. 3(b), which shows the energy-loss spectrum observed in 1.8-keV collisions of $O_2{}^+$ with neutral H_2 molecules. It is pertinent to note that the instrument function in all the present measurements was symmetric in shape; the ratio of signal obtained at all energy-loss values higher than $\Delta E = 0$ with H_2 present in the collision cell to that obtained in the absence of any collision gas was always larger than a factor of about 40. When experiments were carried out with CO^+ projectile ions, once again only excitation of the CO^+ projectiles is observed. Figure 4 shows the energy-loss spectrum of CO^+ obtained in 1.8-keV CO^+-H_2 collisions. The expected energy loss [21] for excitation of the projectile CO^+ from the ground electronic state $^2\Sigma^+$ to $B\,^2\Sigma^+$, $C\,^2\Sigma^+$, and $D\,^2\Pi$ states is indicated in the top portion of Fig. 4.

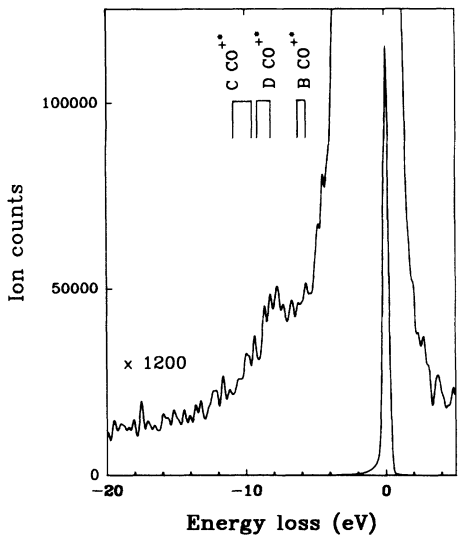

FIG. 4. Energy-loss spectrum of CO^+ ions colliding with H_2 molecules. The excitation energy for vertical excitations to the $B\,^2\Sigma^+$, $C\,^2\Sigma^+$, and $D\,^2\Pi$ states of CO^+ are indicated in the top portion of the figure.

We attempt to rationalize our experimental results using the following simple molecular orbital arguments. The collisional excitation cross section is a function of the overlap of the HOMO's of the two colliding systems and therefore the larger the overlap integral, the larger the resulting collisional excitation cross section. In the case of projectile ions having $^2\Sigma^+$ symmetry ($H_2{}^+$, $N_2{}^+$, and CO^+ projectile ions), the HOMO is a σ_g orbital which has substantial overlap with the HOMO of H_2, which is also σ. Consequently, the energy-loss envelope due to the excitation of the projectile ions, or due to excitation of the target molecule, is only observed in the case of those collisions which involve projectiles that have Σ symmetry. In the case of projectile ions having $^2\Pi$ symmetry ($O_2{}^+$ and $CO_2{}^+$), the HOMO is a π_g^* orbital and the overlap

TABLE III. Calculated values of the magnitude of the overlap integral I for different projectile ions colliding with H_2 in the orientation depicted in Fig. 6 using O_2 as an example. The impact parameter b is varied while c, the horizontal distance between the center of masses, is held fixed at $c = 0$ Å.

b(Å)	$I(H_2{}^+$-$H_2)$	$I(N_2{}^+$-$H_2)$	$I(CO^+$-$H_2)$	$I(O_2{}^+$-$H_2)$	$I(CO_2{}^+$-$H_2)$
2.0	0.539	0.280	0.333	0.00	0.00
3.5	0.145	0.098	0.145	0.00	0.00
5.0	0.024	0.018	0.037	0.00	0.00
6.5	0.004	0.002	0.006	0.00	0.00

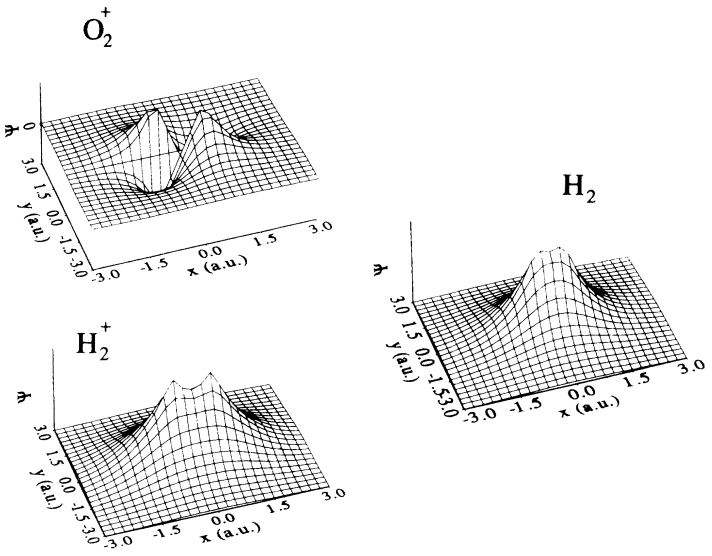

FIG. 5. Plot of the wave functions of the HOMO's of H_2^+, O_2^+, and H_2.

of this with the HOMO of H_2 is very poor. Consequently, neither excitation of the projectile nor excitation of the target is observed in energy-loss spectra measured for such collision systems [as shown in Fig. 3(b)].

In Fig. 5 we have plotted the wave functions of the HOMO's of the H_2 target molecule and H_2^+ and O_2^+ projectile ions. These wave functions are obtained from linear combinations of Gaussian atomic wave functions at the equilibrium internuclear separation of each molecular species. The coefficients for the linear combinations were obtained from self-consistent-field Hartree-Fock calculations carried out by us using a 6-311G** basis set [22]. In order to present a semiquantitative assessment of the differences in the values of overlap integrals for the different collision systems studied in the present experiments, we calculated the overlap integrals at a few crucial orientations of each colliding system. Figure 6 shows the orientation in which the C_∞ axis of the two colliding systems are held parallel to each other at an impact parameter b and the horizontal distance between the center of mass of the projectile ion and the target molecule is denoted by c. Table III shows the overlap integrals of the HOMO's of the colliding systems, with c set at zero and the impact parameter b varied. Table IV shows the overlap integrals obtained when the impact parameter b=3 Å while c is varied. The calculated overlap integrals are seen to be in semiquantitative conformity with the experimental results.

Over and above the molecular orbital considerations discussed above, the fact that excitation of the H_2 target is observable only in the collisions with H_2^+ projectiles is due to the following energy considerations. The vertical excitation energy of target H_2 for the first excited state $^3\Sigma_u^+$, is about 9 eV. It is very probable that collisions resulting in transfer of 9 eV to the target molecule would also result in considerable excitation of the projectile ions. Both N_2^+ and CO^+ have predissociating states whose vertical excitation energy is less than 8 eV [8,20]. Therefore, we postulate that the collisions resulting in excitation of the target H_2 would also result in the excitation of the projectile ions to their predissociating states, leading to their subsequent dissociation. Consequently, such events would not be recorded in the energy-loss spectrum shown in Figs. 3(a) and 4, where it is the kinetic energy of the projectile molecular ions that is monitored. On the other hand, the vertical excitation energy of the first excited state of H_2^+ is about 11.6 eV, which is larger than the excitation energy of H_2 from the ground state to the first excited state and thus in this case excitation of the target H_2 is indeed observed.

TABLE IV. Calculated values of the magnitude of the overlap integral I for different projectile ions colliding with H_2 in the orientation depicted in Fig. 6 using O_2^+ as an example. The impact parameter b is held fixed at b=3 Å while c, the horizontal distance between the center of masses, is varied.

c (Å)	$I(H_2^+$-$H_2)$	$I(N_2^+$-$H_2)$	$I(CO^+$-$H_2)$	$I(O_2^+$-$H_2)$	$I(CO_2^+$-$H_2)$
-2.0	0.147	0.120	0.242	0.051	0.035
-1.0	0.212	0.144	0.247	0.041	0.026
0.0	0.240	0.149	0.202	0.00	0.00
1.0	0.212	0.144	0.141	0.041	0.026
2.0	0.147	0.120	0.086	0.051	0.035

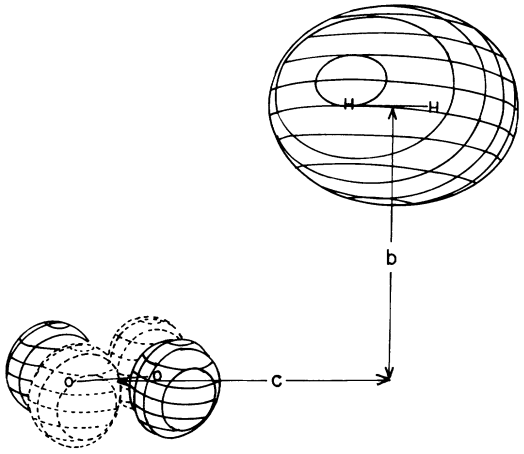

FIG. 6. Plot of the approach of O_2^+ projectiles towards the H_2 target molecule at an impact parameter b; the horizontal distance between the H atom of H_2 and the O atom of O_2^+ is c.

IV. CONCLUSION

In summary, high-resolution translational energy spectrometry has been applied to studies of the excitation of H_2 in 1.8-keV collisions with H_2^+, N_2^+, CO^+, O_2^+, and CO_2^+ projectiles. Excitation of the target to a large number of excited neutral states, as well as to H_2^+ states, is observed in the case of collisions involving H_2^+ projectiles. Franck-Condon integrals for excitation to repulsive electronic states are calculated by the time-dependent wave-packet dynamics approach and compared with the simple calculations using the reflection approximation. The experimental energy-loss envelope is simulated by using convolution techniques and the relative oscillator strength for the excitation to the different states is deduced. Only excitation of the projectile ions is observed in the case of collisions with N_2^+ and CO^+ projectiles. In the case of collisions with O_2^+ and CO_2^+, neither projectile ion excitation nor target molecule excitation is observed. The results are understood in terms of simple molecular orbital arguments and energy considerations.

ACKNOWLEDGMENTS

It is a pleasure to acknowledge U.T. Raheja's expert contributions to the design and fabrication of the translational energy spectrometer. Useful discussions with V.R. Marathe and E. Krishnakumar are gratefully acknowledged.

[1] C. J. Latimer, Adv. At. Mol. Phys. **30**, 105 (1992).
[2] C. Bergnes, D. Bordenave-Montesquieu, A. Boutonnet, P. Nouet, and R. Dagnac, J. Phys. B **19**, 3065 (1986).
[3] Y. Teraoka, T. Ishikawa, and H. Inouye, J. Phys. B **17**, 4911 (1984).
[4] J. H. Black, Adv. At. Mol. Phys. **25**, 477 (1988).
[5] K. P. Kirby and E. F. van Dishoeck, Adv. At. Mol. Phys. **25**, 437 (1988).
[6] A. Dalgarno and T. L. Stephens, Astrophys. J. Lett. **160**, L107 (1870).
[7] D. Dowek, D. Dhuicq, V. Sidis, and M. Barat, Phys. Rev. A **26**, 746 (1982); V. Pol, J. George, and J. T. Park, Bull. Am. Phys. Soc. **18**, 1516 (1973).
[8] M. Krishnamurthy and D. Mathur, J. Phys. B **27**, 1172 (1994).
[9] M. Krishnamurthy and D. Mathur, Int. J. Mass Spectrom. Ion Processes **132**, 137 (1994).
[10] M. Krishnamurthy and D. Mathur, J. Phys. B (to be published).
[11] M. Krishnamurthy, U. T. Raheja, and D. Mathur, Pramana J. Phys. **41**, 271 (1993).
[12] T. E. Sharp, At. Data **2**, 119 (1971).
[13] R. J. LeRoy, University of Waterloo Chemical Physics Research Report No. CP-330, 1991 (unpublished).
[14] H. D. Hagstrum and J. Tate, Phys. Rev. **59**, 354 (1941).
[15] M. Krishnamurthy and D. Mathur, Chem. Phys. Lett. **216**, 203 (1993).
[16] E. J. Heller, Acc. Chem. Res. **14**, 368 (1981).
[17] N. E. Henriksen, J. Zhang, and D. G. Imre, J. Chem. Phys. **89**, 5607 (1988).
[18] R. Kosloff, J. Phys. Chem. **92**, 2087 (1988).
[19] P. Gross, D. Neuhauser, and H. Rabitz, J. Chem. Phys. **96**, 2834 (1992).
[20] A. Lofthus and P. H. Krupenie, J. Phys. Chem. Ref. Data **6**, 113 (1977).
[21] P. Baltzer, M. Carlsson Göthe, B. Wannberg, and L. Karlsson, Rev. Sci. Instrum. **62**, 638 (1991).
[22] W. J. Hehre, Leo Radom, Paul V. R. Schleyer, and John A. Pople, *Ab Initio Molecular Orbital Theory* (Wiley, New York, 1986).